A Comparison of Accuracy of Image- versus Hardware-based Tracking Technologies in 3D Fusion in Aortic Endografting

Alexander E. Rolls[1,2], Blandine Maurel[1], Meryl Davis[1], Jason Constantinou[1], George Hamilton[1], Tara M. Mastracci[1,2]

[1] Aortic Team, Department of Vascular Surgery, Royal Free London Foundation Trust, Pond Street, London NW3 2QG

[2] University College London

Corresponding Author: Tara Mastracci, Aortic Team, Royal Free London NHS Foundation Trust, NW3 2QG
Email: tara.mastracci@nhs.net

Key Words: Fusion, Aneurysms, Image-Based Tracking, Accuracy, Automatic, Registration, Endovascular

Category: original article

Short Statement of Influence in Clinical Practice.

Fusion imaging is recognized as an important tool in complex aneurysm repair to improve the success of implantation and decrease radiation dose and contrast use. It has been previously impossible to compare accuracy of fusion systems because they require fixed hardware, but a new cloud-based system is now available. We compare the accuracy of two different types of fusion imaging. If confirmed, these preliminary results could change clinical practice by encouraging further development of automated image base tracking fusion process.

33

ABSTRACT

Objectives

Fusion of three-dimensional (3D) computed tomography (CT) and intra-operative 2D imaging in endovascular surgery relies on manual rigid co-registration of bony landmarksand tracking of hardware to provide a 3D overlay (Hardware based tracking, HWT). An alternative technique (Imaged based tracking, IMT) uses image recognition to register and place the fusion mask. We present preliminary experience with an agnostic fusion technology that uses IMT, with the aim of comparing the accuracy of overlay for this technology with HWT.

Method

Data was collected prospectively for 12 patients. All devices were deployed using both IMT and HWT fusion-assistance concurrently. Post operative analysis of both systems was performed by 3 blinded expert observers, from selected time-points during the procedures, using the displacement of fusion rings, the overlay of vascular markings and the true ostia of renal arteries. Mean overlay error as well as deviation from mean error was derived using image analysis software. Comparison of mean overlay error was made between IMT and HWT. Validity of the point-picking technique was assessed.

Results

IMT was successful in all of the first 12 cases, whereas technical learning curve challenges thwarted HWT in four cases. When independent operators assessed the degree of accuracy of the overlay, the median error for IMT was 3.9 mm (IQR; 2.89-6.24, max 9.5), versus 8.64 mm (IQR; 6.1-16.8, max 24.5) for HWT (p=0.001). Variance per observer was 0.69 mm^2 and 95% limit of agreement +/- 1.63.

Conclusion

In this preliminary study, the error of magnitude of displacement from 'true anatomy' during image overlay in IMT was less than for HWT. This confirms that

ongoing manual re-registration, as recommended by the manufacturer, should be performed for HWT systems to maintain accuracy. The error in position of the fusion markers for IMT was consistent, thus may be considered predictable.

INTRODUCTION

Endovascular interventions have expanded the treatment opportunities available to patients with aortic disease and have become progressively complex.[1–3] When repair includes coverage of the visceral aortic segment, accurate device deployment and efficient catheterization of target vessels is critical. Fluoroscopic techniques require frequent contrast administration and high quality image recording (DSA) to visualize key structures, resulting in exposure of the patient and surgeon to considerable radiation,[4] and may be associated with deterioration in renal function.[5,6]

Endovascular image fusion refers to the process of merging pre-operative imaging with intra-operative imaging to provide a 3D vascular mask.[7,8] Several studies using commercially available devices have documented variable reduction in radiation exposure, and significant reduction in contrast usage.[9–12] All commercially available systems to date use hardware based tracking to position the mask on the fluoroscopic image. Not all fixed imaging systems require cone beam CT (CBCT) to perform fusion imaging, but at our institution, CBCT is used to create an intraoperative 3D volume that is co-registered with pre-operative imaging. The CBCT data provides the basis for a 3D co-ordinate reference frame that is automatically registered with fluoroscopic imaging, but also incorporates positional data for the vascular landmarks acquired on pre-operative imaging. By combining both soft and bony landmarks for registration, this technique should be superior to those using registration of bony landmarks alone. The position of the image intensifier and operating table are tracked with respect to the co-ordinate reference frame, allowing for appropriate vascular landmark representation when the fluoroscopic image is changed.[13,14] The reliability of this technique depends on the accuracy of "hardware tracking" and the stability of the patient's position on the table once rigid co-registration has been performed.[15] Furthermore, considerable user interaction is required to define the vascular landmarks on a workstation pre-operatively,

manually register the images, and correct registration errors intra-operatively that may arise from patient movement.

A fully automated, image-based 2D-3D registration system that is independent of imaging system manufacturer has been proposed by Carrell et al, and its initial use was described in 2010.[16] This system provides several advantages including being suitable for any theatre even those equipped with mobile C-arm; it is radiation and contrast free for the initial registration; and being fully automated makes it "user friendly" for the operator. The drawback of IMT is that it can only perform fusion on +/-30 degree angles from a standard AP view, and it does require additional equipment to be installed in theatre.

The aim of this study is to compare the accuracy of the fusion overlay between two systems that use different mechanisms to maintain accurate overlay of vascular markings: hardware tracking, and image-based tracking. Because most fusion systems are brand-specific, there has been no previous simultaneous comparison of accuracy between systems on the same patient in the same conditions. Thus, we sought to compare the accuracy of an initial manual registration, followed by hardware tracking using a commercially available device, against continuously updated image-based matching in an investigative device.

MATERIALS AND METHODS

All patients undergoing aortic repair between July 2015 and September 2015 by the Aortic Team at Royal Free London were included in this study. These patients were enrolled in a pre-market trial of CYDAR software and signed consent for involvement. The study was approved by NHS England (IRAS ID 158839) and was closed on September 30, 2015 in accordance with the approved protocol.

All patients with aneurysms underwent pre-operative high-resolution computed angiography (CTA) as standard of care. All patients received stent-graft deployments with fusion assistance using two different systems: a pragmatic application of a

commercially available device that uses hardware tracking (Siemens Artis Zeego, Siemens Healthcare, Erlangen, Germany) and a novel image-based device the Cydar EV system (Cydar Medical, Cambridge, UK) in order to allow for a comparison between the two systems. Fusion would be considered successful if the initial images were available and assisted the surgical procedure. Fusion would be considered a failure if no mask appeared on the screen, or if the position of the mask was so far removed from reality that it was not helpful in the opinion of the operating team.

Hardware-Tracking Fusion Protocol

A hardware-tracking fusion protocol for complex aortic repair has been used at Royal Free London since October 2014. Prior to CBCT, the surgical team imports the pre-operative CTA onto the theatre-based workstation and marked the target vessels by drawing rings at the level of the vessel ostia using Syngo^{TM} (Siemens Healthcare, Erlangen, Germany) software. After induction of general anaesthetic and after all adjustments are made to the patient's position, the patients are fully prepared and draped to minimize any extraneous patient movement after registration. All staff retreat to a shielded and sterile control room prior to CBCT. A 5sDR (5 second acquisition, taking 133 frames at 30 frames/sec) is used for all procedures. Rigid co-registration of the pre-operative CTA with the bony CBCT volume is then performed by the surgeon or an expert radiographer through a manual process. Target vessel rings are assessed intra-operatively on the fluoroscopy screen. Manual re-adjustments of the fusion overlay was not performed since we sought to compare the accuracy of automatic image overlay in both systems after initial co-registration.

Image-based Tracking Fusion Protocol

For each patient the Cydar EV system was also used to generate vascular landmarks which were viewable on an additional screen. Segmentation of the aorta and relevant visceral vessels was performed from the DICOM data of CTA using a semi-automatic method (thresholding followed by region growing), and then rings were manually drawn on the rendered surface by the software provider prior to the day of surgery. The software provider requires 24 hours to prepare the overlay mask. The

software then applies a computational algorithm on pre-operative CT volume to generate a series of images (digitally reconstructed radiographs, [DRRs]) that mimic fluoroscopic images across a range of C-arm rotations and magnifications to match vertebral bodies in both images. An intensity-based registration algorithm then scans the DRR series for images with similar pixel distributions, and automatically matches the most appropriate DRRs to the live fluoroscopic images throughout the procedure. During each fluoroscopic position, the tracking software analyzes the visualized field and attempts to identify vertebrae. If two or more vertebrae are identified, the vascular overlay image created from CT angiography is projected. The algorithm assumes there is a rigid relationship between CT and fluoroscopy, since registration is based on vertebral bodies, and does not adjust for changes in spinal position.[17] The system works when the C-arm is angulated within 30^0 craniocaudally and 40^0 in an anterior-oblique direction, which is a range chosen by the manufacturer that represents a balance between working range of the system and speed of registration.

Error Analysis

Evaluation of error in terms of displacement of fusion rings, or overlaid vascular markings, and the true ostia of the renal arteries on the fluoroscopy screen was the principal measure in this study, which required expert assessment of the true anatomy. We enlisted the observations of three blinded expert observers to identify the location of true renal arteries in each projection. For each case, fluoroscopic screen shots containing representations of renal artery fusion markers for each fusion system were saved and loaded for post-hoc analysis into RView image-analysis software (https://www.doc.ic.ac.uk/~dr/software/; Imperial College London) which was provided to us by the engineers at CYDAR. In order to provide data in millimetres, calibration was performed in each case against longitudinal rigid landmarks on either a calibrated catheter or between two gold markers on a fenestration. For patients receiving fenestrated grafts, conversion of pixels into millimetres was performed using known diameters of fenestrations (either 6 or 8 mm), by measuring the number of pixels against this known dimension (figure 1a).

For patients receiving standard infra-renal grafts conversion was performed in the same manner using the longitudinal markings of a standard measuring pig-tail catheter (distance between each marker: 10 mm). In both scenarios, fluoroscopic images were chosen with measurement markings close to the centre of the screen. Since soft tissues are not visible on fluoroscopy, observers were asked to pick their best estimate of the centre of the renal ostia using images of the fully deployed graft with bridging stents in situ (figure 1b). They were then asked to pick the centre of the fusion markers derived from both the hardware-tracking (figure 1c) and image-based matching (figure 1d) systems. This process was performed for both renal arteries in each case. For the standard infra-renal endovascular aneurysm repair (EVAR) cases, three endovascular observers independently selected the centre of the renal vessel ostium on the basis of the pre-deployment digital-subtraction angiogram. They then selected the centre of the fusion marker. This point picking procedure was repeated with three different observers to provide three error recordings. The RView analysis software provides positional data in the form of pixel co-ordinates for each selected point (x and y). Euclidean principles were used to calculate the distance, in pixels, between the centre of the renal ostia and the fusion markers (as selected by the observers), and was referred to as "error". After conversion to millimetres, each case therefore contained data for two renal arteries, each of which was comprised of three error recordings per fusion system used, that was averaged to give a single mean error value per renal artery, for each fusion system used.

Statistical Analysis

Analysis was performed on SPSS 22.0 (IBM corporation, Chicago, Ill). Data was treated in the following manner: For each renal fusion marker (hardware- and image-tracked), mean values for error in 'x' and 'y' dimensions and error magnitude were calculated across the three observers. Additionally, the difference to mean error magnitude (for all three observers) for each renal was calculated for each observer. Analysis using Pearson's second skewness coefficient found the data to be not-normally distributed. Therefore, in order to compare the distributions in mean error magnitude between the two groups, a non-parametric test was used for un-

paired continuous variables (Mann-Whitney U). To determine if there were any significant differences between the expert "point-pickers", or observers, a Kruskal Wallis test was performed comparing all recorded errors grouped according to expert observer. To determine inter-observer variance and limits of agreement, a Bland Altman-type analysis was used,[18] plotting the mean magnitude of error across the three observers against difference to mean magnitude for each observer. P values of less than 0.05 were considered significant. Calculation of measurement variations were performed with the assistance of engineers at CYDAR imaging.

RESULTS

Between July 2015 and September 2015, twelve patients underwent endovascular repair under general anaesthesia for aortic aneurysms of varying morphology (Table 1) and consented to inclusion in this trial. Seven patients underwent fenestrated endovascular aneurysm repair (FEVAR). Of these patients, four were group IV thoracoabdominal and three were juxtarenal aneurysms. Five patients received infrarenal EVAR, of which three also received iliac branched devices for iliac artery aneurysms. Two patients received coil embolization of the internal iliac on the contralateral side to the branched device. One patient had an isolated iliac aneurysm treated in the presence of a previous endograft with type Ib failure. Mean age for the cohort was 71.9 years (Standard Deviation (SD) 9.7 years). Median aneurysm sac size (aortic or iliac as appropriate) was 6.1 cm (SD 1.1cm). Details of preoperative demographics and intraoperative variables are described in Table 1

All patients underwent successful aneurysm exclusion. Mean procedure time from first entering theatre to leaving theatre was 373 minutes (SD 92m) for fenestrated cases and 220 minutes (SD 45m) for iliac branch cases. The best estimate of procedure time collected at our institution is time from first dose of heparin and first dose of protamine, and for fenestrated cases was 192 minutes (SD 63m); this data was not available for iliac branch cases.

Image Fusion Reliability

The simultaneous overlay of image- and hardware-based tracking in the same patient was feasible in most patients included in the study, and a representative example is shown in figure 2. In the twelve patients included in this study, image-based tracking was successful in all cases and hardware-based tracking was successful in 8 patients. In two patients for which hardware-based tracking was unsuccessful, no fusion overlay appeared intra-operatively, whilst in a further patient the fusion markers were grossly misaligned, and rotated by 90^0 in relation to the true orientation of the aorta. This required manual re-adjustment of the hardware-tracked overlay, and the data was therefore excluded from final statistical analysis. In these cases, failure of hardware-based tracking was due to operator error, and not manufacturing defect, during the workflow of manual registration. In a fourth patient, hardware-based tracking was not possible due to a concurrent update in the hospital's picture archiving and communication system (PACS), preventing image transfer of the pre-operative CTA necessary for 3D rendering and drawing of fusion markers. For IMT cases, all had successful overlay masks projected, and the delay for each different projection was less than 10 seconds for 55% of registrations, and was less than 14 seconds for 92% of registrations.

The mean magnitude of error (figure 3) for the hardware-based tracking system was 8.64 mm (IQR; 6.1-16.8, max 24.5), compared with 3.9 mm (IQR; 2.89-6.24, max 9.5) for the image-based system (p=0.001). Figure 4 gives a positional representation of the distribution of overlay errors registered on the coordinate system described in the methods section. The symbols indicate the direction in which the overlay needs to move in order to match the intra-operative renal position. The image-based overlay markers were consistently located below and mostly on the right side of the true vessel ostium. In contrast, the hardware-tracking based overlay errors were of a greater magnitude, particularly in lateral directions, and located above and below the true vessel ostium. The inter-observer reliability of the blinded "point-picking" technique used by expert observers was good, with the variance per observer in this study being 0.69 mm and the 95% limit of agreement being +/- 1.63 mm, as indicated in the Bland Altman-type plot in figure 5.

DISCUSSION

This is the first preliminary study to compare accuracy of two different types of fusion imaging techniques applied to the same patient undergoing aortic repair. We observe a significant reduction in fusion overlay error (3.9 mm (IQR; 2.89-6.24, max 9.5) compared with 8.64 mm (IQR; 6.1-16.8, max 24.5) (p=0.001)) using a technique that relies on image, rather than hardware for tracking in complex and simple endovascular aortic procedures. The agreement between observers for this error was good.

The use of a similarity-based measure to match digitally reconstructed radiographs to real radiographs, using lumbar vertebrae as a means for rigid 2D-3D image registration was initially proposed by Penney et al in 1998,[19] but was not used clinically due to limitations in fluoroscopic imaging techniques. A more recent study describes the use of a prototype version of the Cydar EV system in a series of retrospective registrations of pre-operative CT-angiograms with archived fluoroscopic images, again using lumbar vertebrae as anchor-points for rigid 2D-3D image registration.[16] The authors observed a mean error of 4.5 +/- 2.8 mm across a total of 98 registrations. Using a newer iteration of the software in this study, we observed a median error of 3.99 mm across 21 renal targets, which was superior to hardware-based image tracking in a pragmatic trial. In the current market place, both GE and Phillips now have proprietary methods for performing 2D-3D fusion without use of a CBCT. In contrast, the routine use of CBCT-based fusion in complex aneurysm repair began as early as 2009 at the Cleveland Clinic, and has enjoyed clinical use in many centres since that time.[9] Removing the CBCT from the process of fusion imaging may have the benefit of decreasing radiation dose while continuing to provide accurate image guidance, however all systems still base tracking on hardware which is subject to inaccuracy if the patient moves.

There was a consistency to errors in image-based tracking that did not appear in hardware-based tracking. All errors appear to portray a slightly lower level of renal arteries. This observation is consistent with findings by Maurel et al, who evaluated the displacement of key visceral arteries by comparing pre-operative CTA with intra-

operative contrast enhanced CBCT, and found that both renal arteries were predominantly displaced in a superior and left direction following the introduction of stiff endovascular instruments.[20] This seems to be true independent of the side of large sheath access, which was different between Maurel et al's experience and our own.. The impact of endovascular tools on soft tissue deformation was suggested by Carrell et al as a possible reason for increased error during image-based registration when the aortic neck was angulated beyond 30^0, since these relatively inflexible devices tend to "straighten out" the aorta.[16] Parallax or differences in body position compared with CT scan protocol could also account for this error. By comparison, inaccuracies due to respiratory movement are thought to be of lesser significance, particularly at the vessel origin.[21,22]

We observed errors of greater magnitudes during hardware-tracked fusion, particularly in lateral directions, as well as errors occurring above and below the intra-operative renal artery origin. These may be accounted for by the fundamental differences in registration technique utilized by the two systems. In theory, the continued and automated image-based matching ought to prevent errors relating to patient movement from occurring, since the system corrects for this by automatically overlaying the most appropriate DRR matched directly to the patient. In contrast, the hardware-tracked system adjusts its representation of fusion markers according to tracked movement of the C-arm and table in a 3D coordinate system, on the assumption that the patient has remained static within that coordinate system after initial rigid co-registration of bony landmarks on has taken place. Our practice was to perform CBCT and the initial registration prior to performing open surgical groin cut-downs, thereby minimizing the risk of contamination. It is plausible that patient movement during this phase and during other manoeuvres that move the patient, such as brachial punctures, may have contributed to the broader distribution of registration errors. Where possible, the team was cautious to maintain the position of the patient throughout the procedure, but despite this attention to detail, the movement was still observed. The authors of this study acknowledge that instructions for use for the Artis Zeego clearly recommend manual adjustment of the overlay following any manipulation or

movement of the patient. In practice, this would require a surgeon to leave the operating theatre and sterile field to use the workstation, or the continued presence of a trained radiographer with experience of using the system, which is not pragmatic in our practice. The work flow for such a protocol is less intuitive and may introduce greater error. The intention of the study was to evaluate the overlay accuracy of both systems when a "hands-off" protocol was applied during the procedure, and to describe the impact of insensible movement on the accuracy of fusion. The finding that patient movement did likely effect hardware based tracking to a greater extent than imaged based tracking suggests that image based tracking may be more resistant to the patient movement in a non-anesthetized patient, which will be a point for future research.

Hardware-tracked fusion failed in 4 patients, which is due to user error, but reflects the multistep process entailed in this technique. In two instances, fusion markers did not appear on the fluoroscopic screen, whilst in a third case the markers were grossly rotated by 90^0 in relation to the orientation of the aorta. In the fourth patient, loss of communication of the PACS system rendered the overlay inaccessible. These failures reflect the cumbersome process that hardware-based tracking currently involves, with many different variables that might impact the workflow. Registration in these cases was performed by senior radiographers who had received intensive training on two separate sessions, each of two days in length. Despite adequate training, the complexity of the registration work-flow seemingly requires operators with a large amount of experience and regular exposure for it to run seamlessly.

It is possible to compare these systems on factors other than accuracy. Certainly in its current form, the HWT system has a larger working range and uses proprietary software which precludes the installation of additional hardware into the operating theatre. Drawbacks of the image-tracked system include the time the registration process takes intra-operatively: each change in C-arm rotation requires a new match to be made between the fluoroscopic image and a DRR which takes several seconds. In some instances this matching cycle needs to be repeated, resulting in a delay

between the change in view and an appropriate overlay of up to 14 seconds. At present, the system does not automatically register when the C-arm is angulated beyond 30^0 and 40^0 in cranio-caudal and anterior-oblique directions, respectively. Whilst sufficient for visualization and cannulation of renal targets, cannulation of mesenteric and coeliac vessels using lateral views and fusion guidance is not possible with the present iteration of the software. Work is presently in progress to expand the scope of available DRRs to enable registration during more angulated fluoroscopic acquisitions. Until that time, use of both systems to augment data available intraoperative seems most prudent.

This is one centre's first attempt at use of image-based tracking, and comprises very early experience. As such, there are a number of limitations to this study. Small numbers of patients in this study could have adversely affected the level of significance observed, and a larger study may provide a more accurate evaluation of the true benefit of this technology. Defining the true centre of the vessel ostia in the fenestrated cases presented a challenge, since it is our practice not to perform pre-deployment DSA and to minimize the use of contrast injections when cannulating the target vessels. We relied instead on using three expert observers to make best estimates with the fenestrated piece fully deployed and the bridging stents in situ, since this provided the most accurate representation of the position of the renal arteries. However, placement of the device could have contributed to the movement of the vessel ostia. Analysis of the distribution of recorded errors in relation to mean error, however, demonstrated a small amount of variance between observers and narrow limits of agreement, suggesting reliability of this method. The lack of data describing patient movement during the procedure is an unfortunate weakness, since the affect of patient movement on the magnitude and direction of overlay inaccuracies in both systems cannot be fully determined. We used as a reference distance the known diameters of the fenestrations for the fenestrated cases, and the calibrated pigtail catheter for the infrarenal cases. We believe in most cases these were perpendicular to the angle of the beam. However, this technique could have a lack of precision and be slightly shorter than expected. For instance for the infrarenal cases if the pigtail catheter is not strictly vertical; or for the

fenestrated cases if the lateral anterior and posterior markers are not on an horizontal line, then the distance between the top and the bottom markers of the window may not correspond to the highest and the lowest points. Finally, we did not take into account neck angulation and renal ostia position on a clockwise that could modify displacement after the insertion of the delivery system and consequently the measurements.

CONCLUSION

Synchronous fusion using two different techniques was feasible, and allowed for a direct comparison of overlay accuracy for image-based and hardware tracking systems. In this very preliminary study, errors in fusion overlay associated with image-based tracking seem predictable and are of a smaller magnitude compared with those observed in a pragmatic application of a hardware-tracked device. Additionally, a major benefit from the image-based fusion is that it does not require a pre-operative CBCT and could help in decreasing the radiation exposure. Further investigation with a larger series is warranted

ACKNOWLEDGEMENTS

We are grateful for the assistance of Dr. Graeme Penney from CYDAR imaging for introducing us to the comparative software and assisting with the measurement technique. Representatives from either fusion system were not consulted for the final draft of this paper.

Conflict of Interest

TMM is a proctor and consults for Cook Medical, as well as speaking arrangements with Maquet Getinge Group. JC has spoken on behalf of Maquet Getinge Group. The CYDAR team helped facilitate the measurements performed.

REFERENCES

1. Mastracci TM, Eagleton MJ, Kuramochi Y, Bathurst S, Wolski K. Twelve-year results of fenestrated endografts for juxtarenal and group IV thoracoabdominal aneurysms. J Vasc Surg 2015; 61:355–364 .
2. Haulon S, D'Elia P, O'Brien N, Sobocinski J, Perrot C, Lerussi G, et al. Endovascular repair of thoracoabdominal aortic aneurysms. Eur J Vasc Endovasc Surg 2010; 39:171–178.
3. Bicknell CD, Cheshire NJ, Riga CV, Bourke P, Wolfe JH, Gibbs RG, et al. Treatment of complex aneurysmal disease with fenestrated and branched stent grafts. Eur J Vasc Endovasc Surg 2009; 37(2):175–181.
4. Kirkwood ML, Arbique GM, Guild JB, Timaran C, Chung J, Anderson JA, et al. Surgeon education decreases radiation dose in complex endovascular procedures and improves patient safety. J Vasc Surg 2013; 58(3):715–721.
5. Kristmundsson T, Sonesson B, Dias N, Törnqvist P, Malina M, Resch T. Outcomes of fenestrated endovascular repair of juxtarenal aortic aneurysm. J Vasc Surg 2014; 59(1):115–120.
6. Martin-Gonzalez T, Pinçon C, Maurel B, Hertault A, Sobocinski J, Spear R, et al. Renal Outcomes Following Fenestrated and Branched Endografting. Eur J Vasc Endovasc Surg 2015; 50(4):420-30.
7. Kaladji A, Dumenil A, Castro M, Haigron P, Heautot JF, Haulon S. Endovascular aortic repair of a postdissecting thoracoabdominal aneurysm using intraoperative fusion imaging. J Vasc Surg 2013; 57(4):1109–1112.
8. Kobeiter H, Nahum J, Becquemin JP. Zero-contrast thoracic endovascular aortic repair using image fusion. Circulation 2011; 124(11):e280–282.
9. Dijkstra ML, Eagleton MJ, Greenberg RK, Mastracci TM, Hernandez A. Intraoperative C-arm cone-beam computed tomography in fenestrated/branched aortic endografting. J Vasc Surg 2011; 53(3):583–590.
10. Hertault A, Maurel B, Sobocinski J, Martin Gonzalez T, Le Roux M, Azzaoui R, et al. Impact of hybrid rooms with image fusion on radiation exposure during endovascular aortic repair. Eur J Vasc Endovasc Surg 2014; 48(4):382–390.
11. Sailer AM, de Haan MW, Peppelenbosch AG, Jacobs MJ, Wildberger JE, Schurink GW. CTA with fluoroscopy image fusion guidance in endovascular complex aortic aneurysm repair. Eur J Vasc Endovasc Surg 2014; 47(4):349–356.

12. McNally MM, Scali ST, Feezor RJ, Neal D, Huber TS, Beck AW. Three-dimensional fusion computed tomography decreases radiation exposure, procedure time, and contrast use during fenestrated endovascular aortic repair. J Vasc Surg 2015; 61(2):309-16.13. Tacher V, Lin M, Desgranges P, Deux JF, Grünhagen T, Becquemin JP, et al. Image guidance for endovascular repair of complex aortic aneurysms: comparison of two-dimensional and three-dimensional angiography and image fusion. J Vasc Interv Radiol 2013; 24(11):1698-1706.

14. Abi-Jaoudeh N, Kobeiter H, Xu S, Wood BJ. Image Fusion During Vascular and Nonvascular Image-Guided Procedures. Tech Vasc Interv Radiol 2013; 16(3):168-76.

15. Varnavas A, Carrell T, Penney G. Increasing the automation of a 2D-3D registration system. IEEE Trans Med Imaging 2013; 32(2):387–399.

16. Carrell TWG, Modarai B, Brown JRI, Penney GP. Feasibility and limitations of an automated 2D-3D rigid image registration system for complex endovascular aortic procedures. J Endovasc Ther 2010; 17(4):527-33.

17. Penney GP, Batchelor PG, Hill DL, Hawkes DJ, Weese J. Validation of a two- to three-dimensional registration algorithm for aligning preoperative CT images and intraoperative fluoroscopy images. Med Phys 2001; 28(6):1024–1032.18. Jones M, Dobson A, O'Brian S. A graphical method for assessing agreement with the mean between multiple observers using continuous measures. Int J Epidemiol 2011; 40(5):1308–1313.19. Penney GP, Weese J, Little JA, Desmedt P, Hill DL, Hawkes DJ. A comparison of similarity measures for use in 2-D-3-D medical image registration. IEEE Trans Med Imaging 1998; 17(4):586–595.

20. Maurel B, Hertault A, Gonzalez TM, Sobocinski J, Le Roux M, Delaplace J, et al. Evaluation of visceral artery displacement by endograft delivery system insertion. J Endovasc Ther 2014; 21(2):339-47.

21. Draney MT, Zarins CK, Taylor CA. Three-dimensional analysis of renal artery bending motion during respiration. J Endovasc Ther 2005; 12(3):380-6.

22. Fukuda T, Matsuda H, Doi S, Sugiyama M, Morita Y, Yamada M, et al. Evaluation of automated 2D-3D image overlay system utilizing subtraction of bone marrow image for EVAR: feasibility study. Eur J Vasc Endovasc Surg 2013; 46(1):75-81.

Figures and Tables

Table 1: Demographics for included patients. *(SD: standard deviation; HTN: Hypertension; DM: diabetes mellitus; CCF: congestive cardiac failure; BMI: body mass index ; GFR: glomerular filtration rate; DAP: dose area product; CAK: cumulative air kerma)*

	N (12)
Age	71.9 years (SD 9.7 yrs)
Male	11/12
Medical Comorbidities	
HTN	12/12
Dyslipidemia	11/12
Current Smoker	2/12
DM	4/12
CCF	2/12
BMI	26.6 (SD 4.9)
Pre op GFR	67.7 (SD 24.7)
Post op GFR	64.8 (SD 23.9)
Aneurysm Characteristics	
Aneurysm sac size	6.1cm (SD 1.08 cm)
Infrarenal Aneurysm	2/12
Iliac Artery Aneurysm	3/12
Juxtarenal aneurysm	3/12
Type IV TAAA	4/12
Intraoperative Variables	
DAP	91.7 Gy.cm^2 (SD 67.92)
KAP	0.78 mGy (SD 0.69)
Volume of Contrast	46cc (SD 14.9)

519

520

521

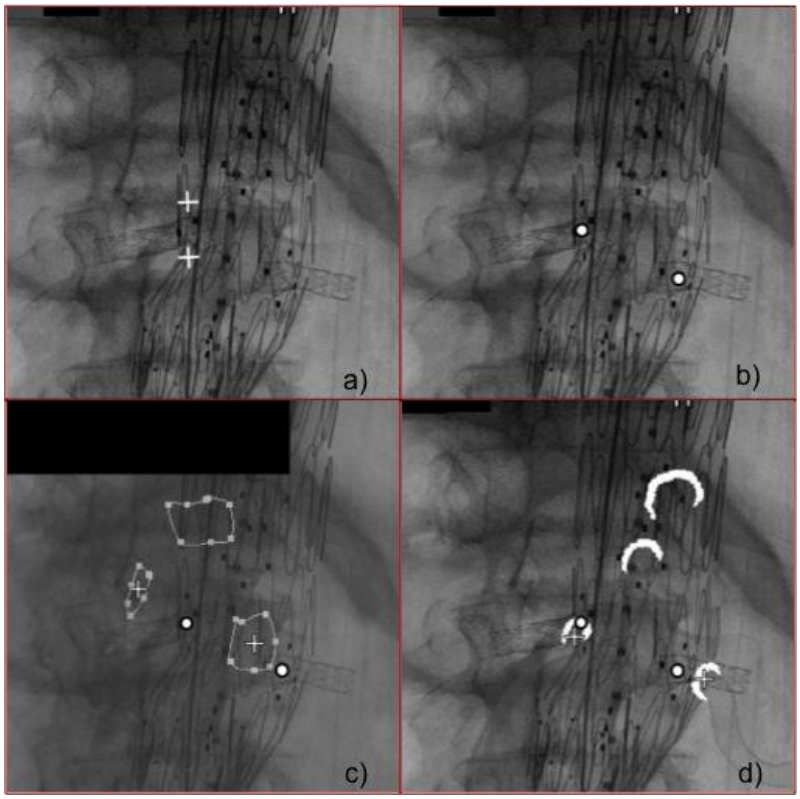

522

523 Figure 1

524

525

526

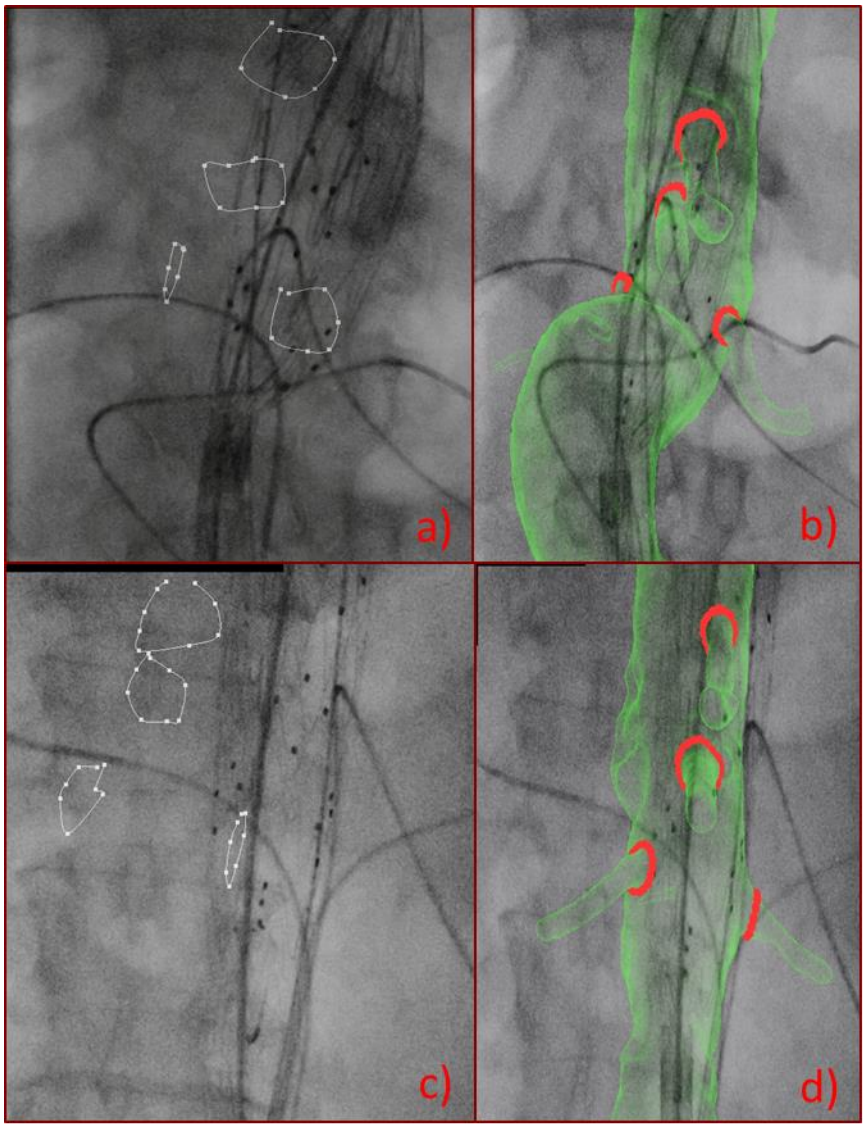

527

528

529 Figure 2

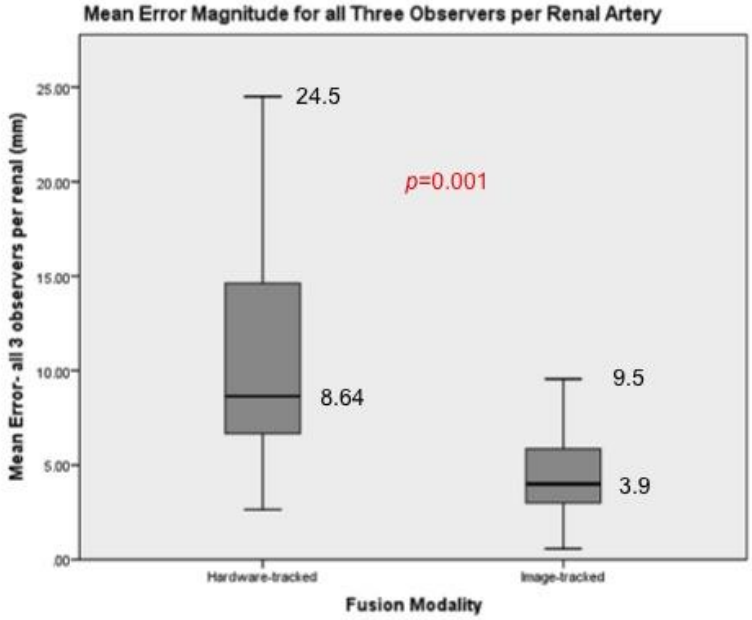

530

531 Figure 3

532

533

534

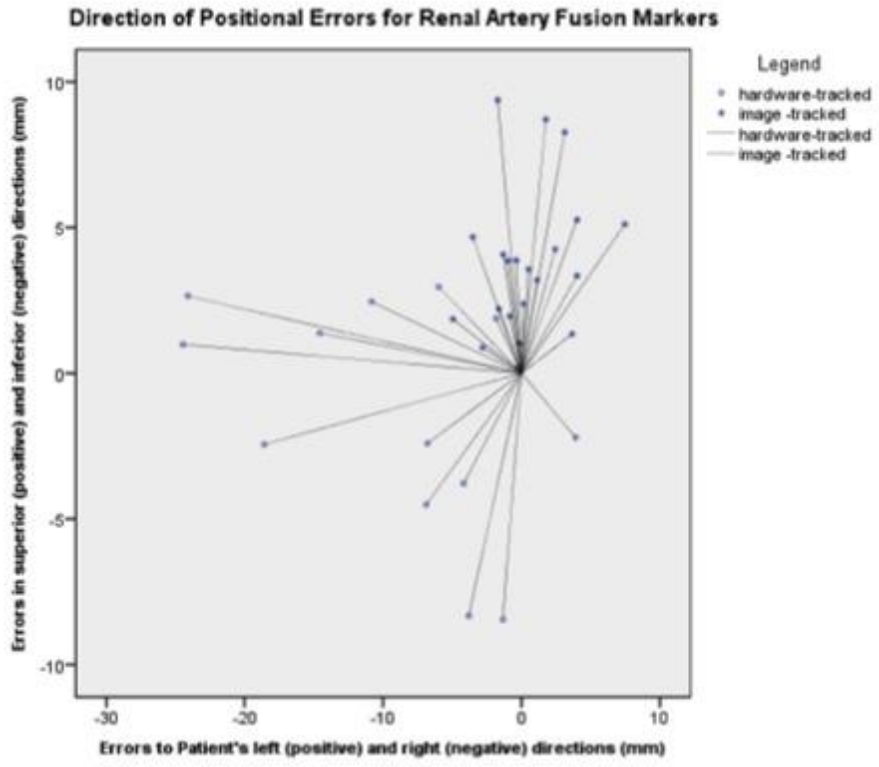

535

536 Figure 4

537

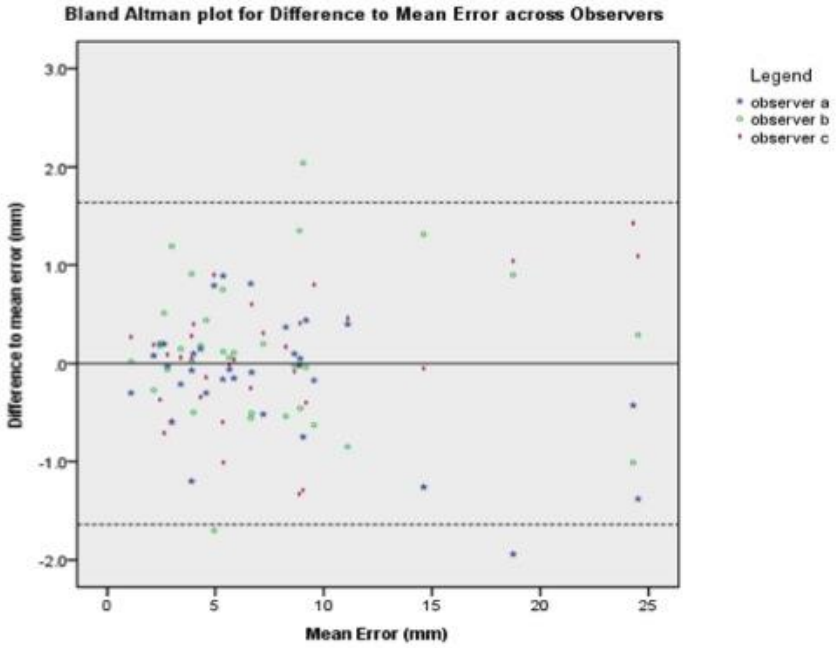

Figure 5

Table and Figure Legend

Table 1: Patient demographics and aneurysm morphology. IA- Iliac artery. IRAAA- infrarenal abdominal aortic aneurysm. EVAR- endovascular aneurysm repair. FEVAR- fenestrated endovascular aneurysm repair. IBD- iliac branched device. Results are expressed in mean and standard deviation (SD). *(SD: standard deviation; HTN: Hypertension; DM: diabetes mellitus; CCF: congestive cardiac failure; BMI: body mass index ; GFR: glomerular filtration rate; DAP: dose area product; CAK: cumulative air kerma)*

Figure 1: Calibration and Point-selection a) Conversion of pixels into mm, in this case the known dimensions of a fenestration. b) Centre of the renal ostium is selected. c)

Centre of the hardware-tracked fusion marker is selected d) Centre of the image-tracked fusion marker is selected

Figure 2: Hardware-based tracking and Image-based tracking fusion systems applied to two cases, with each row representing the same case. a) and c)- hardware-based tracking. b) and d)- image-based tracking

Figure 3: Comparison of mean error magnitude for all three observers per renal artery, by fusion system used.

Figure 4: Scatter-plot showing mean error per renal artery in x and y coordinates. The symbols pointing away from the origin represent the direction in which the overlay would have to be moved to match the actual vessel ostium.

Figure 5: Bland Altman-type plot showing deviation from the mean error for each renal artery. Each data point represents the difference between an observer's recorded overlay error during point selection to the mean overlay error recorded for all three observers for a given renal artery. The dotted lines represent the 95% limits of agreement.